Article:
Sieber, J., Wagg, D.J. and Adhikari, S. (2008) On the interaction of exponential non-viscous damping with symmetric nonlinearities. Journal of Sound and Vibration, 314 (1-2). 1 - 11. ISSN: 0022-460X

https://doi.org/10.1016/j.jsv.2007.12.017

Journal of Sound and Vibration (2008) 314 (2008) 1–11

On the interaction of exponential non-viscous damping with symmetric nonlinearities

J. Sieber [a], D. J. Wagg [b,*], and S. Adhikari [c]

[a] *Department of Engineering, University of Aberdeen, Aberdeen, Scotland AB24 3UE, U.K.*

[b] *Department of Mechanical Engineering, University of Bristol, Queens Building, University Walk, Bristol BS8 1TR, U.K.*

[c] *School of Engineering, University of Swansea, Swansea, SA2 8PP, U.K.*

Abstract

This paper studies the interaction between non-viscous damping and nonlinearities for nonlinear oscillators with reflection symmetry. The non-viscous damping function is an exponential damping model which adds a decaying memory property to the damping term of the oscillator. We consider the case of softening and hardening behaviour in the frequency response of the system. Numerical simulations of the Duffing oscillator show a significant enhancement of the resonance peaks for increasing levels of non-viscous damping parameter in the hardening case, but not in the softening case.This can be explained in the general context by an energy balance analysis of the undamped unforced oscillator, which shows that for hardening nonlinearities the growth of damping with the energy level is an order of magnitude smaller in the exponential case than in the viscous case.

Key words: damping, Duffing, exponential, non-viscous.

1 Introduction

Viscous damping is the most common model for modelling of vibration damping. This model, first introduced by Lord Rayleigh [1], assumes that the instantaneous generalised velocities are the only relevant variables that determine damping. Viscous damping models are used widely for their simplicity and

* Corresponding author.
Email address: David.Wagg@bristol.ac.uk (D. J. Wagg).

mathematical convenience even though the behaviour of real structural materials may not be adequately represented by viscous models [2]. For this reason it is well recognised that in general a physically realistic model of damping is unlikely to be viscous. Damping models in which the dissipative forces depend on any quantity other than the instantaneous generalised velocities are non-viscous damping models [3,4]. Mathematically, any causal model which makes the energy dissipation functional non-negative is a possible candidate for a non-viscous damping model [5, 6]. Clearly a wide range of choice is possible, either based on the physics of the problem, or by *a priori* selecting a model and fitting its parameters from experiments.

In this paper we consider a damping model called the "exponential" damping model, which has been shown to have useful properties for modelling vibration. With this model the damping force is expressed as

$$f_d(t) = \int_0^t c\,\mu e^{-\mu(t-\tau)}\dot{u}(\tau)\,d\tau. \tag{1}$$

Here c is the viscous damping constant, μ is the relaxation (or non-viscous damping) parameter and $u(t)$ is the displacement as a function of time. This model was originally proposed by Biot [7,8] and later used be several authors in the context of dynamics of linear elastic and viscoelastic systems. Equation (1) physically implies that the previous time histories of the velocity $\dot{u}$ contribute to the current damping force and the most recent instances of velocity have the highest influence. In the limiting case when $\mu \to \infty$, the exponential kernel function approaches the Dirac delta function $\delta(t)$. For this special case the damping force given by equation (1) reduces to the case of viscous damping.

One way to view the exponential damping model is as a generalisation of the classical viscous damping model. In this case one could potentially enhance the damping modelling capability of numerical models using the exponential model. Methods for the analysis of linear single-degree-of-freedom [21, 22] as well as multiple degree-of-freedom systems [3–6, 19, 20] with damping of the form (1) have been considered. The following reasons for the selection of this type of model can be given:

- For viscoelastic systems, an equation similar to (1) is often associated with the stiffness parameter. In this context, the physical basis for exponential models has been well established. Cremer and Heckl [2] concluded that 'Of the many after-effect functions that are possible in principle, only one — the so-called relaxation function — is physically meaningful.'
- It has been noted that when the damping is non-viscous, forceful fitting of viscous damping may produce non-physical result, for example, a non-symmetric coefficient matrix [23]. For linear multiple-degree-of-freedom systems, Adhikari and Woodhouse [24] have proposed a method to identify both the viscous and non-viscous parameters in equation (1) from exper-

imental vibration measurements. This gives significantly improved results over trying to fit a single parameter viscous model to experimental data.

Due to its enhanced damping modelling capabilities, several authors have considered non-viscous damping models in the context of linear single-degree-of-freedom as well as multiple degree-of-freedom systems. Golla and Hughes [9] McTavis and Hughes [4] have proposed a method to obtain equations of motion similar to (1) using a time-domain finite-element formulation. Their approach (the GHM method) introduces additional dissipation coordinates corresponding to the internal dampers. Dynamic responses of the system were obtained by using the eigensolutions of the augmented problem in the state-space. Bishop and Price [10] have considered equations of motion similar to (1) in the context of *ship dynamics*. The convolution term appeared in order to represent the fluid forces and moments. It is worth noting that a related modelling technique used to model non-viscous effects is fractional damping (see for example [12] and references therein). Bagley and Torvik [11], Torvik and Bagley [13], Gaul et al. [14] and Maia et al. [15] have considered damping modelling in terms of fractional derivatives of the displacements. The resulting equation has a convolution integral form similar to equation (1). In the context of engineering vibration, typical applications for non-viscous damping models occur in the study of dampers used for vibration isolation [16], for example, base isolation of buildings [17].

Specifically, in this paper we a consider single-degree-of-freedom oscillator with a symmetric stiffness nonlinearity and varying levels of harmonic forcing. A classical prototype of this type of nonlinear system is the Duffing oscillator with harmonic forcing. In order to understand the effect of adding non-viscous damping to a nonlinear system we focus on the well understood situation of a weak nonlinearity balanced with weak damping (that is, small c in equation (1)). Section 4 discusses the two subcases of weak symmetric stiffness nonlinearity: the hardening (section 4.1) and the softening (section 4.2) nonlinearity.

In short, we find that positive non-viscosity μ induces two qualitative differences. First, we observe a moderate shift in the onset of nonlinear behaviour toward lower forcing amplitudes for increasing μ. This can be explained by the linear analysis of the zero state as found in [21] and summarised in Section 3. Second, and more prominently, large resonance peaks are significantly enhanced for hardening nonlinearities, but not for softening nonlinearities. Our analysis shows that for the exponential force model, equation (1), the growth of dissipation with the energy level is orders of magnitude smaller than for the viscous damping model. This effect must be attributed to the interaction with the nonlinearity which comes into play at large amplitude oscillations. All numerical simulations are carried out using the classical Duffing oscillator, such that we can study the effects of exponential damping using a system with well known nonlinear dynamic behaviour. However, the analysis is indepen-

dent of the particular cubic Duffing-type nonlinearity and, thus, carries over to general symmetric stiffness nonlinearities.

In Section 2 we present the Duffing oscillator, which serves as a prototype for nonlinear single-degree-of-freedom forced oscillators, and introduce non-viscous damping into the model. Non-dimensionalisation leads to a system of three first order differential equations depending on five parameters, of which two relate to the external forcing, one captures the nonlinearity of the stiffness behaviour, one represents the viscous damping and one the non-viscous damping. Then in Section 3 we summarise the theory on the effects of the exponential non-viscous damping model on a linear harmonic oscillator.

Section 4 starts with numerical simulations of the Duffing oscillator, which show a strong effect of non-viscosity for the case with a cubic hardening stiffness term. This includes resonance peaks which can have have unbounded growth in amplitude. We present an energy balance analysis of the undamped and unforced case which we use to demonstrate how the unbounded growth can occur in the hardening case. The same analysis is used to demonstrate that in the softening case the effect of the non-viscosity is relatively minor. Conclusions are drawn in Section 5.

2 The forced Duffing oscillator with non-viscous exponential damping

The Duffing oscillator has been widely studied, and comprehensive reviews of the associated literature can be found in [25–28]. For these type of systems the damping is nearly always assumed to be viscous. Notable exceptions are a study of a Duffing vibration isolator which has combined Coulomb and viscous damping [29] and a study considering the effect of fractional damping on the Duffing oscillator [30]. In addition a preliminary study on the system considered in this paper has been carried out by two of the current authors [31].

Replacing viscous damping by the exponential damping force, equation (1), the governing equation for the forced Duffing oscillator can be expressed as

$$m\frac{\mathrm{d}^2x}{\mathrm{d}\hat{t}^2} + c\int_{\hat{\tau}=0}^{\hat{\tau}=\hat{t}} \mu \mathrm{e}^{-\mu(\hat{t}-\hat{\tau})}\frac{\mathrm{d}x}{\mathrm{d}\hat{\tau}}\mathrm{d}\hat{\tau} + kx + \alpha k x^3 = A\cos(\Omega\hat{t}), \tag{2}$$

where x represents the displacement of the oscillator mass m, the linear stiffness is given by k, the coefficient α, represents the form of the cubic stiffness nonlinearity, $\hat{t}$ is time and $\hat{\tau}$ is the integration variable. The viscous damping coefficient is c and the non viscous damping effects are represented by the parameter μ. The forcing amplitude is $A = x_0 k$, where x_0 is the equivalent static displacement.

Introducing the nondimensional time variables $t = \hat{t}\omega_n$ and $\tau = \hat{\tau}\omega_n$, where $\omega_n = \sqrt{k/m}$ is the natural frequency of the linear part, means that equation (2) can be expressed as

$$\ddot{x} + 2\zeta \int_0^t \frac{\mathrm{e}^{-\frac{1}{\beta}(t-\tau)}}{\beta} \dot{x} d\tau + x + \alpha x^3 = x_0 \cos(\omega t), \tag{3}$$

where $\zeta = c/(2m\omega_n)$, $\beta = \omega_n/\mu$, $\omega = \Omega/\omega_n$ and an overdot represents differentiation with respect to nondimensional time.

We now define the integral term in equation (3) as

$$y = \int_0^t \frac{\mathrm{e}^{-\frac{1}{\beta}(t-\tau)}}{\beta} \dot{x} d\tau. \tag{4}$$

Then by using the Leibniz rule for differentiation of an integral [3] we can write

$$\dot{y} = \frac{1}{\beta}\dot{x} - \frac{1}{\beta}y. \tag{5}$$

We can then write equations (3) and (5) as a set of three first order ordinary differential equations

$$\begin{aligned} \dot{x}_1 &= x_2, \\ \dot{x}_2 &= -2\zeta y - x_1 - \alpha x_1^3 + x_0 \cos(\omega t), \\ \dot{y} &= \frac{1}{\beta}x_2 - \frac{1}{\beta}y, \end{aligned} \tag{6}$$

where all three equations have dimensions of length, which can be scaled out as required. We note that if we multiply through the last line of equation (6) by β, then as $\beta \to 0$, $y \to x_2$ and the viscous damping case is obtained.

The parameters m, c and k are positive for physically realistic oscillators. However, the coefficient α can have positive or negative sign depending on the physical type of nonlinearity.

Setting $|\alpha| \ll 1$ corresponds to the weakly nonlinear cases of hardening (α positive) or softening (α negative) cubic spring behaviour encountered in a range of mechanical applications. For weak nonlinearities we can set α to any particular value (for example, $\alpha = 1$) without loss of generality because different values of α correspond to a rescaling of the state space variables x_1, x_2 and y. For the numerical simulations we have chosen α small such that the forcing is of order one. Alternatively, one may fix x_0 to 1 and vary α as bifurcation parameter. This corresponds to a quadratic rescaling of the y-axis in the numerical bifurcation diagrams 3 and 4.Figure 1 shows the frequency response of these two cases, illustrating the effect of the nonlinearity as the

characteristic "bending" of the resonance peak for non-zero forcing x_0. The resonance peak bends toward the range of higher frequencies in the hardening case (a) whereas it bends toward lower frequencies in the softening case (b). If the forcing exceeds a critical value, defined as $x_{0,c}$, the bending gives rise to the appearance of two limit points (called LP in Figure 1) and a region of bistability between these two limiting frequencies. Typically the "upper" limit point (ULP) is close to the resonance peak and frequency.

The sections 4.1 and 4.2 study how the presence of a nonzero exponential non-viscous damping coefficient β affects characteristic expressions of the nonlinearity, namely the size of the region of bistability, the critical forcing $x_{0,c}$, and the height and location of the resonance peak.

3 Effects of exponential damping on a linear oscillator

The equation of motion of a linear single-degree-of-freedom system with damping characteristics given by equation (1) can be expressed as

$$\ddot{x} + 2\zeta \int_{\tau=0}^{\tau=t} \frac{\mathrm{e}^{-\frac{1}{\beta}(t-\tau)}}{\beta} \dot{x}(\tau)\mathrm{d}\tau + x = f(t), \tag{7}$$

together with the initial conditions

$$x(0) = x_0 \quad \text{and} \quad \dot{x}(0) = \dot{x}_0. \tag{8}$$

Qualitative properties of the eigenvalues of this system have been discussed in detail by Adhikari [21,22]. Here we review some basic results which are useful in understanding the results of the nonlinear system discussed in section 4.

Transforming equation (7) into the Laplace domain one obtains

$$s^2\,\overline{x}(s) + \left(\frac{2\zeta\, s}{s\beta + 1}\right)\overline{x}(s) + \overline{x}(s) = \overline{f}(s) + \dot{x}_0 + \left(s + \frac{2\zeta}{s\beta + 1}\right) x_0, \tag{9}$$

where s is the complex Laplace domain parameter and $\overline{(\bullet)}$ is the Laplace transform of $(\bullet)$. When $\zeta \to 0$ the oscillator is effectively undamped. When $\beta \to 0$ then the oscillator is effectively viscously damped. In what follows, we will use these limiting cases to develop a physical understanding of the results to be derived in Section 4.

Manipulation of equation (9) and substituting $s = i\omega$, [21], enables a non-dimensional frequency response function to be expressed as

$$G(i\omega) = \frac{1 + i\beta\omega}{(1 - \omega^2) + i\omega\,(2\zeta + \beta - \beta\omega^2)}. \tag{10}$$

From equation (10), the amplitude of vibration can be obtained as

$$|G(i\omega)| = \sqrt{G(i\omega)\, G^*(i\omega)} = \sqrt{\frac{1+\beta^2\omega^2}{\left(1-\omega^2\right)^2 + \omega^2\left(2\zeta+\beta-\beta\omega^2\right)^2}}. \qquad (11)$$

Figure 2 shows the amplitude of the non-dimensional frequency response $|G(i\omega)|$ as a function of the normalised frequency ω. The numerical values of β and ζ are selected such that Figure 2 represents the general overall behaviour. The amplitude of vibration is scaled such that it is equal to one in the static case, that is, when $\omega = 0$. Therefore as the frequency changes, the values of $|G(i\omega)|$ in equation (11) can be regarded as the amplification factors. When β is less than a critical value β_c [21], such that $\beta < \beta_c = 1/(3\sqrt{3})$ the frequency response function is similar to that of the viscously damped system. This is expected because the value of β is relatively small.

For all cases in Figure 2, we observe that the amplitude of the peak response of the non-viscously damped system is higher than that of the viscously damped system. In general the higher the value of β, the higher the value of the amplitude of the peak response. This is due to the fact that the real part $\mathrm{Re}[s]$ of the dominant weakly damped complex eigenmode pair of the linear oscillator, equation (7), increases from $\mathrm{Re}[s] = -\zeta$ to $\mathrm{Re}[s] \approx -\zeta/2$, moving closer to the imaginary axis, for β increasing from 0 to 1 [21]. The eigenvalues of the oscillator, equation (7), correspond to the complex roots of the denominator of $G(i\omega)$. This means that an increase of β corresponds to a decrease of the effective damping. A similar effect is caused by including an integral term in a feedback control law. We can expect that this decrease of effective damping at the linear level causes nonlinear effects to become observable at smaller forcing amplitudes (which is indeed the case, see Section 4).

Another interesting observation in Figure 2 is that the dynamic response amplitude has a peak even when $\zeta > 1/\sqrt{2}$. For example, in Figure 2(d), the viscously damped system does not have any response peak as $\zeta = 1$ (critical viscous damping). However, for the non-viscously damped system, the response amplitude has a peak when $\beta = 1$ or $\beta = 0.75$, but not if $\beta < 0.5$. See reference [22] for an in-depth exploration of these response behaviours.

4 Analysis of the interplay between nonviscous damping and nonlinearity

4.1 The effect of non-viscous damping on systems with hardening nonlinearities

The hardening stiffness nonlinearity, $\alpha > 0$ in equation (3) is characterised by a bending of the resonance peak toward the high-frequency end. The illustration in Figure 1(a) shows that, for forcing amplitudes x_0 larger than the critical amplitude, $x_{0,c}$, this bending of the resonance peak causes a region of bistability, bounded by two limit points. Figure 3(a) depicts how this region of bistability in the (ω, x_0)-plane depends on the non-viscous damping coefficient β. The other two relevant parameters have been kept fixed at a small value: $\alpha = 0.05$ and (without loss of generality) $\zeta = 0.05$. The region of bistability in the (ω, x_0)-plane typically has the form of a wedge with a cusp $(\omega_c, x_{0,c})$ that is pointing downwards. The cusps of all curves are marked by grey-filled circles in Figure 3(a) (partially obscuring each other and effectively forming a line). For each value of β from 0.1 to 1 (varying in steps of size 0.1) the diagram in Figure 3(a) shows the curves of limit points bounding this wedge of bistability (compare also Figure 1(a)). The part of each curve bounding a wedge of bistability from the right corresponds to the ULP in Figure 1(a), which is for moderately large forcing amplitudes ($x_0 > x_{0,c}$) very close to the top of the resonance peak. This implies that the location of the top of the resonance peak coincides (approximately) with the right boundary of the bistability region (the curve emanating to the right from the cusp in Figure 3(a)), at least for parameter values far from the cusp. The part of the curve bounding the wedge of bistability from the left corresponds to the LLP in Figure 1(a). The location of LLP in parameter and phase space is virtually unaffected by β: all LLP curves in Figure 3(a) lie on top of each other.

The wedge shape of the bistability region and the curves of limit points are known for the classical viscous case ($\beta = 0$). As Figure 3(a) indicates, they persist also for non-viscous damping ($\beta > 0$). However, there are two qualitative changes. First, the cusp $(\omega_c, x_{0,c})$ is shifted downwards when increasing β from 0 to 1 (see inset of Figure 3(a)). That is, the larger the non-viscous damping β the smaller the critical forcing amplitude $x_{0,c}$ that causes the resonance peak to bend enough for bistability. The inset in Figure 3(a) zooms into the parameter region of the cusps, showing only the cusps as a curve $(x_{0,c}(\beta), \omega_c(\beta))$ for β varying in the interval $[0, 1]$. The explanation for the downward shift of $x_{0,c}$ follows from the analysis of the unforced non-viscous system, linearised around zero. Section 3 showed that, for the linear oscillator system, we have a decrease of effective damping for increasing β. Lower effective damping causes nonlinear effects to become observable at smaller forcing

amplitudes. This implies that one would expect the cusp to shift down to the parameter region of smaller forcing amplitude, which indeed occurs.

The second, more prominent, effect of non-viscous damping is the widening of the region of bistability (see Figure 3(a)). More precisely, for every $\beta > 0$ there exists a second critical forcing amplitude $x_{0,\infty}$ for which the top of the resonance peak disappears toward $\omega = +\infty$ and infinite amplitude $\max_{\{t\}} x_1(t) = \infty$. The limit points on the curves to the right of the cusp in Figure 3(a), which correspond to the ULPs, are close to the top of the resonance peak if the resonance peak itself is large (compare the top of the peak and the upper limit point, denoted ULP, in Figure 1(a)). Thus, the location of the right curve of limit points in Figure 3(a) is a good approximation for the top of the resonance peak as well.

Figure 3(b) focuses on the asymptotic behaviour of the ULPs which are approximately at the top of the resonance peak. The figure shows the limit point curve for large ω, plotting it in the parameter plane period $(2\pi\omega^{-1})$ vs. $x_0\beta^2$, which is a transformation of the (ω, x_0)-plane in Figure 3(a). It can be seen that the limit point curves stay finite for $\omega \to \infty$, indicating that a scaling law exists of the form $x_{0,\infty} \sim \beta^{-2}$. This implies that for $x_0 > x_{0,\infty}(\beta)$ one will not find the large sharp bent resonance peak of Figure 1(a). Instead the response amplitude always increases for increasing ω, coexisting with a small amplitude response for all $\omega > \omega_1(\beta)$, the left "lower" limit point (LLP).

One can understand this qualitative difference to the viscous case by considering the forced weakly damped system, equation (6) as a small forcing/small damping perturbation of the conservative unforced oscillator

$$\begin{aligned} \dot{x}_1 &= x_2, \\ \dot{x}_2 &= -x_1 - \alpha x_1^3. \end{aligned} \tag{12}$$

This consideration is certainly valid for large amplitude responses as they occur near the high (and very sharp) resonance peaks. The oscillator, equation (12) preserves the energy $h(x) = (x_2^2 + x_1^2)/2 + \alpha x_1^4/4$. Each energy level $h \geq 0$ corresponds to a (free-phase) periodic orbit of equation (12) with a unique frequency $\tilde{\omega}(h)$. The function $\tilde{\omega}(h)$ increases strictly monotonically due to the hardening type of the nonlinearity. Let us denote its inverse by $\tilde{h}(\omega)$. A high amplitude response of the forced and damped system in equations (6) follows as a zero order approximation a periodic orbit $\gamma = (x_1(t), x_2(t))$ of equation (12) corresponding to a certain energy level h. This orbit γ and its energy level h are determined by two criteria, a *resonance* condition and a *phase* (or balance) condition. The resonance condition states that

$$\tilde{\omega}(h) = \omega \quad \text{or, equivalently,} \quad h = \tilde{h}(\omega) \tag{13}$$

where ω is the forcing frequency. The resonance condition, equation (13) fixes

the energy level h of the response for a given forcing frequency ω to $\tilde{h}(\omega)$ due to the monotonicity of $\tilde{\omega}$ and $\tilde{h}$. The phase condition states that the integral of

$$\begin{aligned}\dot{h} &= \frac{\partial h}{\partial x_1}\dot{x}_1 + \frac{\partial h}{\partial x_2}\dot{x}_2, \\ &= -2\zeta x_2(t)y(t) + x_0 x_2(t)\cos(\omega t),\end{aligned} \tag{14}$$

equals zero along the periodic orbit $\gamma = (x_1(t), x_2(t))$ of equation (12) corresponding to the energy level h:

$$0 = \int_\gamma \dot{h} = \int_\gamma -2\zeta x_2(t)y(t) + x_0 x_2(t)\cos(\omega t)\, dt. \tag{15}$$

The phase condition means that the phase of the orbit is determined such that the damping $-2\zeta \int_\gamma x_2 y$ and the forcing $x_0 \int_\gamma x_2 \cos(\omega t)$ balance each other. In equation (14) y is the unique periodic solution of $\beta\dot{y}(t) = x_2(t) - y(t)$ (for the viscous case $\beta = 0$ we simply have $y(t) = x_2(t)$).

The phase condition, equation (15) can be recast by introducing the phase explicitly as a new parameter ϕ (without loss of generality we put ϕ into the forcing and assume that $x_2(0) = 0$, $x_1(0) = \sqrt{2\tilde{h}(\omega)}$) such that

$$\begin{aligned}2\zeta \int_\gamma x_2(t)y(t) &= x_0\cos(\phi)\int_\gamma x_2(t)\cos(\omega t) - x_0\sin(\phi)\int_\gamma x_2(t)\sin(\omega t) &(16)\\ &= -x_0\sin(\phi)\int_\gamma x_2(t)\sin(\omega t). &(17)\end{aligned}$$

The first term on the right-hand-side of equation (16) vanishes because the nonlinearity (and, thus, x_2) is odd. The right-hand-side of equation (17) varies for $\phi \in [0, 2\pi]$ between $\pm x_0 \int_\gamma x_2(t)\sin(\omega t)$. Consequently, the following criterion determines the existence of exactly two different high amplitude responses of the weakly damped and weakly forced system, equation (6):

$$\left| 2\zeta \int_0^{2\pi/\omega} x_2(t)y(t)\, dt \right| < \left| x_0 \int_0^{2\pi/\omega} x_2(t)\sin(\omega t)\, dt \right| \tag{18}$$

where $(x_1(t), x_2(t))$ is the periodic orbit of the conservative oscillator on the energy level $\tilde{h}(\omega)$ starting from $(x_1(0), x_2(0)) = (\sqrt{2\tilde{h}(\omega)}, 0)$, and y is the unique periodic solution to $\beta\dot{y} = x_2 - y$.

For the viscous case we have $y(t) = x_2(t)$ in equation (18). This implies that the left side of equation (18) grows much faster in h (and ω) than the right side. Indeed, $|\int_\gamma x_2 \sin(\omega t)|$ equals the modulus $|x_{2,1}|$ of the first Fourier coefficient of x_2 whereas $\int_\gamma x_2^2(t)$ equals $\sum_{k=-\infty}^{\infty} x_{2,k}^2$, the sum of the squares of all Fourier coefficients. Thus, for a certain, sufficiently large, forcing frequency ω

inequality (18) will turn into an equality. At this frequency ω and its energy level $\tilde{h}(\omega)$ we have the resonance peak and the ULP. For larger forcing frequencies damping dominates the forcing such that there is no high amplitude response.

For positive β, however, the term $\int_\gamma x_2(t)y(t)$ is orders of magnitude smaller than $\sum_{k=0}^{\infty} x_{2,k}^2$. In fact, for large ω,

$$\int_0^{2\pi/\omega} x_2(t)y(t) = \sum_{k=-\infty}^{\infty} \frac{x_{2,k}^2}{1+i\omega\beta k} \ll \sum_{k=-\infty}^{\infty} x_{2,k}^2 = \int_0^{2\pi/\omega} x_2^2(t). \qquad (19)$$

Consequently, modelling with exponential damping will always lead to predictions that have a significant enhancement of large resonance peaks for hardening nonlinearities. This observation and criterion, equation (18), are independent from the particular Duffing type cubic nonlinearity of equation (6) and the modulus of parameter α.

In the case of the Duffing oscillator studied here we observe that $\sqrt{2\tilde{h}(\omega)} \sim \omega$, $|x_{2,1}| \sim \omega$, $\int_\gamma x_2(t)^2 \sim \omega^2$ and $\int_\gamma x_2(t)y(t) \sim \omega$. This implies the existence of the critical forcing amplitudes $x_{0,\infty}$ which we observed in Figure 3(b).

4.2 The effect of non-viscous damping on nonlinearities of softening type

The softening nonlinearity ($\alpha < 0$) is characterised by a bending of the resonance peak toward the low-frequency end. This causes a region of bistability in the (ω, x_0)-plane which has a wedge shape similar to the hardening case but flipped toward the low-frequency end. Figure 4 shows how this region of bistability depends on the non-viscous damping coefficient β. In panel (a) all bistability wedges for $\beta = 0.1$ to 1 (in steps of size 0.1) have been projected onto the (ω, x_0)-plane. Panel (b) shows a 3d-view of the full parameter space (ω, x_0, β). Clearly, the dependence on β in this case is relatively minor. One observes a shift of the cusp toward lower forcing amplitudes similar to the hardening case due to the effects of the non-viscous damping on the effective damping in the linearisation of the zero state. At large amplitudes there is no noticeable effect of the increase of β. This can be explained by arguments similar to those employed for high amplitude responses for the hardening case. In equation (19) the difference between the viscous and the nonviscous case lies in the denominator $1 + i\omega\beta k$ where ω is large for hardening nonlinearities but small or moderate for softening nonlinearities. Thus, we cannot expect the exponential damping model to give qualitatively different predictions compared to the classical viscous one.

We remark that the classical Duffing oscillator with purely viscous damping

($\beta = 0$) and a softening nonlinearity exhibits an intricate web of bifurcations for small ω [27], including symmetry breaking and sequences of period doubling leading to chaos. Hence, the unperturbed case $\beta = 0$ shows dynamics in the left part of Figure 4(a) that depends sensitively on initial conditions and all parameters, including β. Changes of these features, however, are too subtle to be clearly attributed to the effect of the inclusion of the exponential damping, which would correspond to an increase of β. Any other parameter variation may effect the same change.

5 Conclusions

In this paper we have considered the dynamics of a weakly nonlinear Duffing oscillator with a non-viscous exponential damping model. This system can be reduced to a set of three ODE's, which can then be simulated numerically. We have considered the cases of softening and hardening behaviour in the frequency response of the system. The numerical simulations show that a significant enhancement of the nonlinear resonance peaks is observed for increasing levels of non-viscous damping parameter in the hardening case, but not in the softening case. This can be explained by an energy balance of the equivalent undamped, unforced (hardening) case, which shows that the growth of exponential damping with the energy level is several orders of magnitude smaller than the growth of viscous damping. As a result damping reduces close to the resonance peak for positive non-viscosity and for sufficiently large forcing, the bistable region becomes infinite. Qualitatively, the conclusion that exponential damping enhances the resonance peak can be generalised to general hardening spring nonlinearities.

6 Acknowledgements

The authors would like to acknowledge the support of the Engineering and Physical Sciences Research Council. Both DJW and SA are currently EPSRC Advanced Research Fellows.

References

[1] J.W.S. Rayleigh. *Theory of Sound*, (two volumes). Dover Publications, (1877).

[2] L. Cremer & M. Heckl. *Structure-Borne Sound*. Springer-Verlag Berlin, Germany, (1973).

[3] N. Wagner & S. Adhikari. Symmetric state-space formulation for a class of non-viscously damped systems *AIAA Journal*, **41**, 951–956, (2003).

[4] D.J. McTavish & P.C. Hughes. Modelling of linear viscoelastic space structures *Transactions of ASME, Journal of Vibration and Acoustics*, **115**, 103–110, (1993).

[5] A. Muravyov & S.G. Hutton. Closed-form solutions and the eigenvalue problem for vibration of discrete viscoelastic systems *Transactions of ASME, Journal of Applied Mechanics*, **64**, 684–691, (1997).

[6] A. Muravyov & S.G. Hutton. Free vibration response characteristics of a simple elasto-hereditary system *Transactions of ASME, Journal of Vibration and Acoustics*, **120**, 628-632, (1998).

[7] M.A. Biot. Variational principles in irreversible thermodynamics with application to viscoelasticity. *Physical Review*, **97**, 1463–1469 (1955).

[8] M.A. Biot. Linear thermodynamics and the mechanics of solids. *Proceedings of the Third U. S. National Congress on Applied Mechanics*, 1–18 (1958).

[9] D.F. Golla & P.C. Hughes. Dynamics of viscoelastic structures — a time domain finite element formulation. *Journal of Applied Mechanics, ASME*, **52**, 897–906 (1985).

[10] R.E.D. Bishop & W.G. Price. An investigation into the linear theory of ship response to waves. *Journal of Sound and Vibration*, **62**, 353–363 (1979).

[11] R.L. Bagley & P.J. Torvik. Fractional calculus—a different approach to the analysis of viscoelastically damped structures *AIAA Journal*, **21**, 741–748 (1983).

[12] L.J. Sheu, H.K. Chen, J.H. Chen & L.M. Tam. Chaotic dynamics of the fractionally damped Duffing equation. *Chaos Solitons & Fractals*, **32**, 1459–1468 (2007).

[13] P.J. Torvik & R.L. Bagley. Fractional derivatives in the description of damping: materials and phenomena. *The Role of Damping in Vibration and Noise Control*, 125–135 (1987).

[14] L. Gaul, P. Klein & S. Kemple. Damping description involving fractional operators *Mechanical Systems and Signal Processing*, **5**, 81–88 (1991)

[15] N.M.M. Maia, J.M.M. Silva & A.M.R. Ribeiro. On a general model for damping *Journal of Sound and Vibration*, **218**, 749–767 (1998).

[16] K.D. Papoulia & J.M. Kelly. Visco-hyperelastic model for filled rubbers used in vibration isolation. *Journal of Engineering Materials and Technology-Transactions of the ASME*, **119**, 292–297 (1997).

[17] C.G. Koh & J.M. Kelly. Application of fractional derivatives to seismic analysis of base-isolated models. *Earthquake Engineering & Structural Dynamics*, **19**, 229–241 (1990).

[18] S. Adhikari & J. Woodhouse. Quantification of non-viscous damping in discrete linear systems *Journal of Sound and Vibration*, **260**, 499-518, (2003).

[19] S. Adhikari. Dynamics of non-viscously damped linear systems *ASCE Journal of Engineering Mechanics*, **128**, 328-339, (2002).

[20] J. Woodhouse. Linear damping models for structural vibration *Journal of Sound and Vibration*,**215**, 547-569, (1998).

[21] S. Adhikari. Qualitative dynamic characteristics of a non-viscously damped oscillator. *Proceedings of the Royal Society A*, **461**: 2269–2288, (2005).

[22] S. Adhikari. Dynamic response characteristics of a non-viscously damped oscillator *Transactions of ASME, Journal of Applied Mechanics: In Press*, (2007).

[23] S. Adhikari. & J. Woodhouse. Identification of damping: part 1, viscous damping *Journal of Sound and Vibration*, **243**, 43-61, (2001).

[24] S. Adhikari. & J. Woodhouse. Identification of damping: part 2, non-viscous damping *Journal of Sound and Vibration*, **243**, 63-88, (2001).

[25] J. Guckenheimer & P. Holmes. *Nonlinear oscillations, dynamical systems, and bifurcations of vector fields*. Springer-Verlag: New York, (1983).

[26] F.C. Moon. *Chaotic vibrations: An introduction for applied scientists and engineers* John Wiley: New York, (1987).

[27] J.M.T. Thompson. & H.B. Stewart. *Nonlinear dynamics and chaos* John Wiley: Chichester, (2002).

[28] A.H. Nayfeh & D.T. Mook. *Nonlinear oscillations* John Wiley: New York, (1979).

[29] B. Ravindra & A.K. Mallik. Hard Duffing type vibration isolator with combined Coulomb and viscous damping *International Journal of Non-linear Mechanics*, **28**, 427-440, (1993).

[30] M. Borowiec, G. Litak & A. Syta. Vibration of the Duffing oscillator: Effect of fractional damping *Shock and Vibration*, **14**, 29-36, (2007).

[31] D.J. Wagg & S. Adhikari. On the Dynamics of a Duffing Oscillator with an Exponential Non-Viscous Damping Model *in Proceedings of the Eighth International Conference on Computational Structures Technology, Civil-Comp Press, Topping, Montero & Montenegro (eds.)*, (2006).

[32] E.J. Doedel, A.R. Champneys, T.F. Fairgrieve, Y.A. Kuznetsov, B. Sandstede, & X. Wang. *AUTO97, Continuation and bifurcation software for ordinary differential equations* Concordia University, (1998).

[33] F. Schilder. *RAUTO: running AUTO more efficiently 2007*. http://www.dynamicalsystems.org/sw/sw/.

Journal of Sound and Vibration (2008) 314 (2008) 1–11

Figure Captions

- Figure 1: Duffing oscillator with non-viscous exponential damping model. Illustration of the effect of (a) hardening and (b) softening nonlinearity on the frequency response. The maximum x_1 value per forcing period is shown against frequency ω. Solid lines denote stable solution branches, and dashed lines are unstable branches. The limit points (LP) are shown as dots. The coefficients are: $\alpha = 0.05$, $x_0 = 2.5$ for (a), and $\alpha = -0.05$, $x_0 = 0.2$ for (b). The damping coefficients are $\beta = 0.05$ and $\zeta = 0.05$ for both diagrams. (Numerical computations carried out with AUTO [32] and RAUTO [33].)
- Figure 2: Linear oscillator with non-viscous exponential damping model. Amplitude of the non-dimensional frequency response $|G(i\omega)|$ as a function of the frequency ω for different values of ζ and β. The frequency ω is normalised to multiples of the natural frequency $\omega_n = \sqrt{k/m}$ of the original system. (a) $\zeta = 0.1$, (b) $\zeta = 0.25$, (c) $\zeta = 0.5$, and (d) $\zeta = 1.0$
- Figure 3: Duffing oscillator with non-viscous exponential damping model. Panel (a): Region of bistability, bounded by curves of limit points, in the (ω, x_0)-plane and their dependence on β. The inset shows the cusps of the bistability regions enlarged for varying $\beta \in [0, 1]$. Panel (b): asymptotics of the limit point curves (and approximate resonance peaks) in the $(2\pi/\omega, x_0\beta^2)$-plane for large ω (that is, small periods). Other parameters: $\zeta = 0.05$, $\alpha = 0.05$. (Numerical computations carried out with AUTO [32] and RAUTO [33].)
- Figure 4: Duffing oscillator with non-viscous exponential damping model. Region of bistability in the (ω, x_0)-plane and their dependence on β (panel (a)) and in the three-dimensional space of the parameters (ω, x_0, β). Other parameters: $\zeta = 0.05$, $\alpha = -0.05$. (Numerical computations carried out with AUTO [32] and RAUTO [33].)

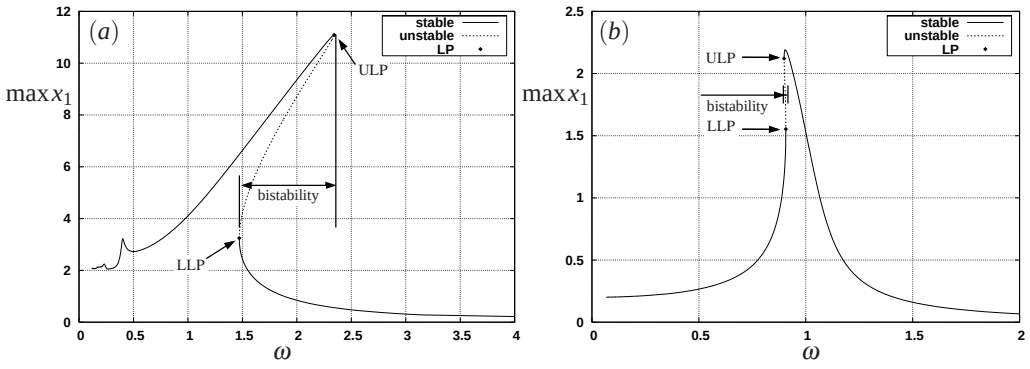
(a)
stable
unstable
LP
ULP
bistability
LLP
max x_1
ω
(b)
stable
unstable
LP
ULP
bistability
LLP
max x_1
ω

Fig. 1.

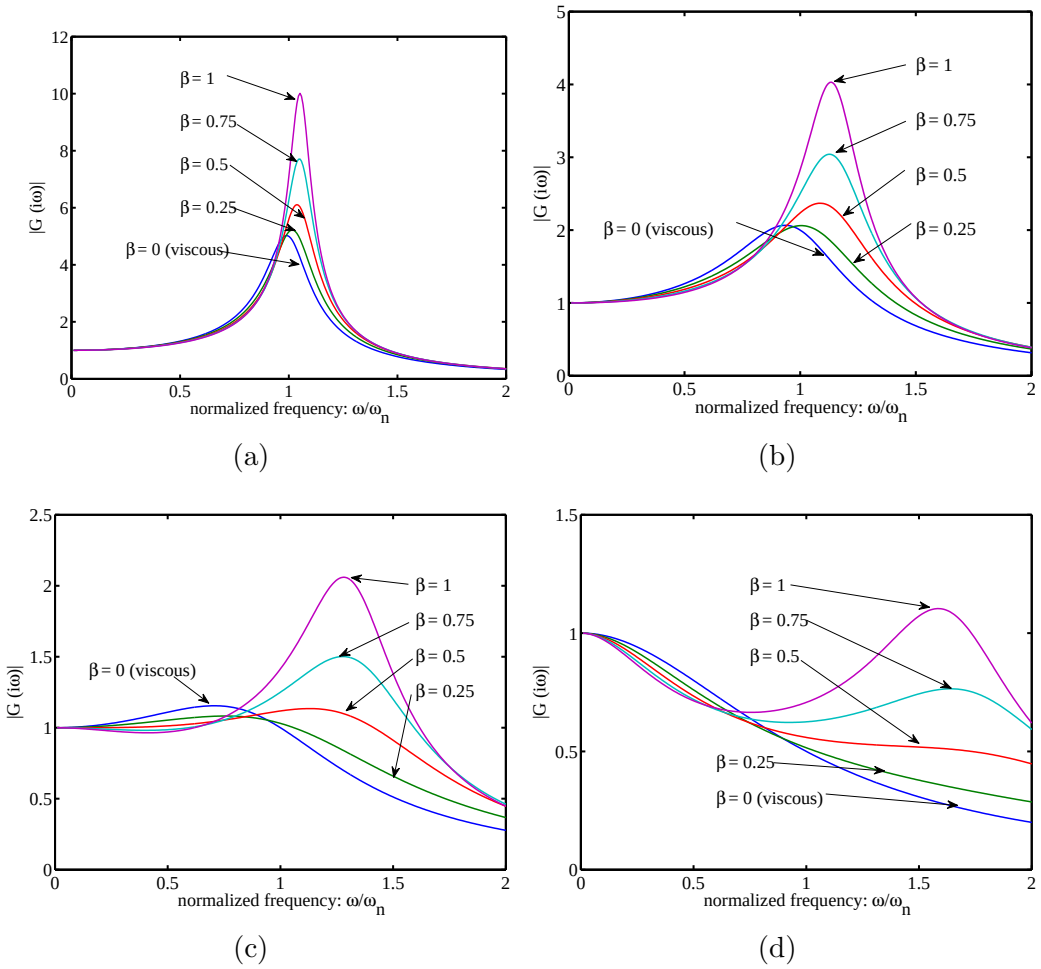
β = 1
β = 0.75
β = 0.5
β = 0.25
β = 0 (viscous)
|G (iω)|
normalized frequency: ω/ω_n
(a)
(b)
(c)
(d)

Fig. 2.

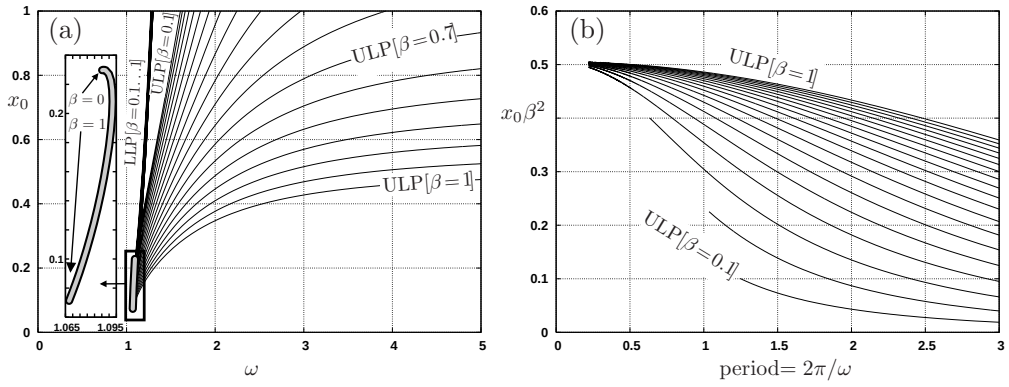
(a)
x_0
ω
ULP[β=0.7]
ULP[β=1]
ULP[β=0.1,..,1]
ULP[β=0.1]
$\beta=0$
$\beta=1$
1.065
1.095
(b)
$x_0\beta^2$
period= $2\pi/\omega$
ULP[β=1]
ULP[β=0.1]

Fig. 3.

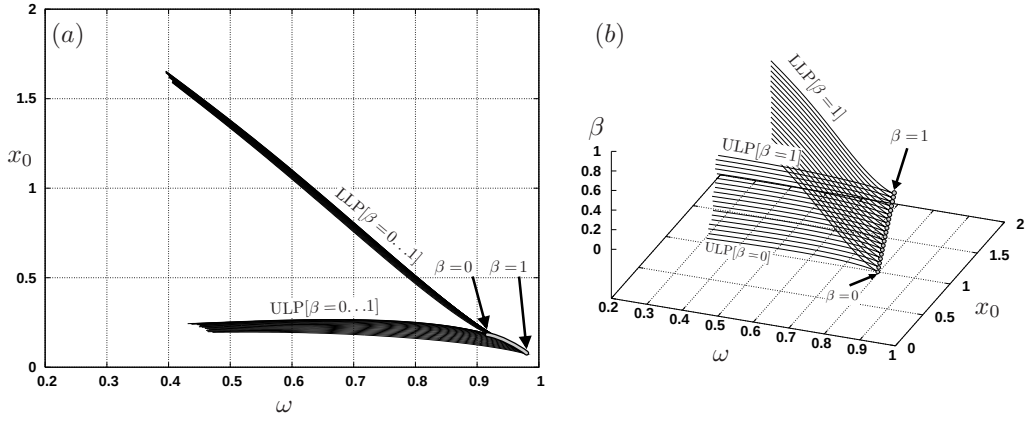
(a)
(b)
x_0
ω
β
LLP[$\beta=0\ldots1$]
ULP[$\beta=0\ldots1$]
$\beta=0$
$\beta=1$
LLP[$\beta=1$]
ULP[$\beta=1$]
ULP[$\beta=0$]

Fig. 4.